

NOAA Technical Memorandum ERL GLERL-32

THE **FREE** OSCILLATIONS OF **LAKE** ST. CLAIR --  
AN APPLICATION OF LANCZOS' PROCEDURE

David J. Schwab

Great Lakes Environmental Research Laboratory  
Ann Arbor, Michigan  
July 1980



**UNITED STATES  
DEPARTMENT OF COMMERCE  
Philip M. Klutznick, Secretary**

**NATIONAL OCEANIC AND  
ATMOSPHERIC ADMINISTRATION  
Richard A. Frank, Administrator**

**Environmental Research  
Laboratories  
Wilmot N. Hess, Director**



## TABLE OF CONTENTS

	Page
Abstract	1
1. INTRODUCTION	1
2. GOVERNING EQUATIONS	1
3. LANCZOS PROCEDURE	3
4. APPLICATION TO LAKE ST. CLAIR	5
5. CONCLUSION	7
6. REFERENCES	12

## FIGURES

	Page
1. Numerical grid for Lake St. Clair. Depth contours at 2-m intervals.	6
2. Amplitude distribution for the first normal mode of Lake St. Clair, with a period of 4.06 h.	9
3. Amplitude distribution for the second normal mode of Lake St. Clair, with a period of 3.12 h.	10
4. Amplitude distribution for the third normal mode of Lake St. Clair, with a period of 2.17 h.	10
5. Amplitude distribution for the fourth normal mode of Lake St. Clair, with a period of 1.89 h.	11
6. Amplitude distribution for the fifth normal mode of Lake St. Clair, with a period of 1.74 h.	11

## TABLE

1. Frequencies of oscillation of Lake St. Clair as determined by the <b>Lanczos</b> procedure at various truncations. Frequencies are in cycles per hour. Asterisks denote spurious <b>eigenvalues</b> as explained in the text.	8
--	---

THE FREE OSCILLATIONS OF LAKE ST. CLAIR--AN APPLICATION OF  
LANCZOS' PROCEDURE'

David J. Schwab

The frequencies and structures of the five lowest free oscillations of Lake St. **Clair** are determined by a Lanczos procedure. With the Lanczos procedure, a high resolution numerical grid can be used to resolve the detailed structures of the modes. The lowest mode has a calculated period of 4.06 h.

1. INTRODUCTION

The purpose of this paper is to present a method of determining the frequencies of free oscillation of an enclosed basin and, more importantly, a high resolution representation of the modal structures. The method used is a Lanczos procedure applied to the linear shallow water equations. The advantage of this procedure is that the governing differential operator can be **discretized** on a high resolution numerical grid without taxing the memory capacity of the computer.

2. GOVERNING EQUATIONS

The linearized, **inviscid** shallow water equations in the absence of rotation and forcing can be written as

$$\frac{\partial \vec{v}}{\partial t} = -g \nabla \zeta \quad (1)$$

and 
$$\frac{\partial \zeta}{\partial t} + \nabla \cdot (h \vec{v}) = 0 \quad , \quad (2)$$

where  $\vec{v}$  is the horizontal velocity vector,  $\zeta$  is the free surface fluctuation,  $h$  is the water depth,  $t$  is the time, and  $\nabla$  is the horizontal gradient operator. The boundary condition is that of perfect reflection, that is,

$$\vec{v} \cdot \vec{n} = 0 \quad (3)$$

at the shoreline. The term  $\vec{n}$  is a vector normal to the shoreline.

---

<sup>1</sup>GLERL Contribution No. 237.

Eliminating  $\vec{v}$  from (1) and (2) to find a single equation for  $\zeta$ , we find

$$\frac{\partial^2 \zeta}{\partial t^2} - g \nabla \cdot h \nabla \zeta = 0 . \quad (4)$$

The boundary condition for  $\zeta$  is, from (1) and (3)

$$\frac{\partial \zeta}{\partial n} = 0 . \quad (5)$$

The free solutions of (4) are

$$\zeta_n(x, y, t) = \eta_n(x, y) e^{i \sigma_n t} . \quad (6)$$

Substituting into (4) and eliminating the time dependent part gives

$$-\sigma_n^2 \eta_n - g \nabla \cdot h \nabla \eta_n = 0$$

or

$$\nabla \cdot h \nabla \eta_n = \lambda_n \eta_n , \quad (7)$$

where the  $n^{\text{th}}$  characteristic value,  $\lambda_n$ , is defined as

$$\lambda_n = \frac{-\sigma_n^2}{g} . \quad (8)$$

To show that  $\lambda_n$  is real and negative, and therefore that  $\sigma_n$  is real so the free solutions are purely harmonic, multiply (7) by  $\eta_n^*$  and integrate over the area of the basin.

$$\int \eta_n^* \nabla \cdot h \nabla \eta_n \, dA = \lambda_n \int \eta_n^* \eta_n \, dA .$$

Partial integration and use of the boundary condition (5) gives

$$\lambda_n = -\int h \nabla \eta_n^* \cdot \nabla \eta_n \, dA / \int \eta_n^* \eta_n \, dA .$$

This shows  $\lambda_n$  to be real and negative.

One can also show the  $\eta_n$  to be orthogonal. Since  $\lambda_n$  is real,  $\eta_n$  is real.

One can write (7) for a different mode  $m$  as

$$\nabla \cdot h \nabla \eta_m = \lambda_m \eta_m. \quad (9)$$

Now multiply (7) by  $\eta_m$ , (9) by  $\eta_n$ , and subtract to obtain

$$\eta_m \nabla \cdot h \nabla \eta_n - \eta_n \nabla \cdot h \nabla \eta_m = (\lambda_n - \lambda_m) \eta_n \eta_m. \quad (10)$$

Integrate (10) over the area of the basin.

$$\int (\eta_m \nabla \cdot h \nabla \eta_n - \eta_n \nabla \cdot h \nabla \eta_m) dA = (\lambda_n - \lambda_m) \int \eta_n \eta_m dA$$

Partial integration of the left side and use of the boundary condition (5) gives

$$(\lambda_n - \lambda_m) \int \eta_n \eta_m dA = 0. \quad (11)$$

If  $m = n$ , this equation is satisfied trivially. For two different characteristic values,  $(\lambda_n - \lambda_m) \neq 0$  so

$$\int \eta_n \eta_m dA = 0. \quad (12)$$

The **eigenfunctions** are orthogonal.

The free solutions to equations (1) and (2) are then characterized by pure harmonic time dependence with frequencies  $\omega_n$  and mathematically orthogonal spatial structures.

### 3. LANCZOS PROCEDURE

To solve (7) for  $\lambda_n$  and  $\eta_n$ , we use a Lanczos procedure. When applied to the **discretized** version of a differential operator, the Lanczos procedure (developed by Lanczos, 1950, and explained more fully in Paige, 1972) results in a **tri-diagonal** matrix with the same **eigenvalues** as the general matrix of the differential operator. To proceed, first expand  $\eta_n$  as follows:

$$\eta_n = \sum_{i=1}^{\infty} C_i^n W_i, \quad (13)$$

where the  $W_i$  are **orthonormal** over the area of the basin and satisfy the same boundary conditions as  $\eta$ , i.e.,

$$\frac{\partial W_i}{\partial n} = 0.$$

The **orthonormality** condition is

$$\int W_i W_j dA = \delta_{ij}, \quad (14)$$

where  $\delta_{ij}$  is the Kronecker delta.

Later the  $W_i$  will be further specified to simplify the calculation. (7) is then

$$\nabla \cdot h \nabla \sum_{i=1}^{\infty} C_i^n W_i = \lambda_n \sum_{i=1}^{\infty} C_i^n W_i. \quad (15)$$

Multiply by  $W_j$  and integrate over the area of the basin.

$$\int W_j \nabla \cdot h \nabla \sum_{i=1}^{\infty} C_i^n W_i dA = \lambda_n \int \sum_{i=1}^{\infty} C_i^n W_i dA \quad (16)$$

Let

$$A_{ij} = \int W_j \nabla \cdot h \nabla W_i dA \quad (17)$$

and use the orthogonality condition (14) to obtain

$$\sum_{i=1}^{\infty} A_{ij} C_i^n = \lambda_n C_j^n$$

or

$$A \vec{C} = \lambda \vec{C}, \quad (18)$$

which is a standard **eigenvalue** problem. Note that **discretizing** the differential operator in (7) would result in the same sort of system as (18). The order of the matrix A would be proportional to the number of grid squares in the digitization of the basin and the structure would be somewhat banded but lacking any symmetric properties. The entire matrix would have to be stored in the computer to obtain eigenvalues and vectors. In the **Lanczos** procedure the  $W_i$  functions are chosen so that the matrix A is symmetric tridiagonal. Special numerical routines described in Smith *et al.* (1974) are used to find the eigenvalues and eigenvectors of the tridiagonal matrix. Only the main diagonal and first off-diagonal of the matrix are stored **in** the computer since the rest of the matrix elements are zero. Let

$$\alpha_i = \int W_i \nabla \cdot h \nabla W_i dA \quad (19)$$

$$\hat{W}_{i+1} = (\nabla \cdot h \nabla - \alpha_i) W_i - \beta_i W_{i-1} \quad i \geq 1 \quad (20)$$

$$\beta_{i+1} = (\int \hat{W}_{i+1} \hat{W}_{i+1} dA)^{1/2} \quad (21)$$

$$W_{i+1} = \hat{W}_{i+1} / \beta_{i+1}. \quad (22)$$

If  $W_1$  is given, (19)-(22) define a recursion relation for  $W_i$ ,  $\alpha_i$ , and  $\beta_i$ . A useful way of writing (20) is

$$\beta_{i+1} W_{i+1} = (\nabla \cdot h \nabla - \alpha_i) W_i - \beta_i W_{i-1}$$

or 
$$\nabla \cdot h \nabla W_i = \alpha_i W_i + \beta_{i+1} W_{i+1} + \beta_i W_{i-1}. \quad (23)$$

Multiply (23) by  $W_j$  and integrate over the area of the basin.

$$\int W_j \nabla \cdot h \nabla W_i dA = \alpha_i \int W_j W_i dA + \beta_{i+1} \int W_j W_{i+1} dA + \beta_i \int W_j W_{i-1} dA \quad (24)$$

We obtain the diagonal elements of A in (18) by letting  $j = i$  in (24).

$$A_{ii} = \int W_i \nabla \cdot h \nabla W_i dA = a_i \quad (25)$$

The first off-diagonal is obtained by letting  $j = i-1$  in (24).

$$A_{i-1 i} = \int W_{i-1} \nabla \cdot h \nabla W_i dA = \beta_i. \quad (26)$$

It is easy to see that the matrix is symmetric

$$A_{i i-1} = \int W_i \nabla \cdot h \nabla W_{i-1} dA = \beta_i \quad (27)$$

and that all other elements are zero.

In summary, the **Lanczos** procedure for the solution to (7) consists of: 1) selecting a starting function  $W_1$ ; 2) applying (19)-(22) recursively to obtain  $\alpha_i$ ,  $\beta_i$  and  $W_i$ ; 3) solving (18) for **eigenvalues**  $\sigma_n$  and **eigenvectors**  $\hat{C}_n$ ; and 4) constructing  $\eta_n$  from (13).

#### 4. APPLICATION TO LAKE ST. CLAIR

The outline and bathymetry of Lake St. Clair are digitized on a 1200-m grid yielding 731 square elements as shown in Fig. 1. The depth plotted in this figure includes a 0.8-m stage above low water datum (an average value for recent years). The recursion procedure (19)-(22) is applied with centered difference formulas for the gradient operator and simple summation for the integrations. Analytically, all the  $W_i$  are orthogonal according to (14). After applying (19)-(22) to the numerical grid 731 times, we should find that  $W_{732} = 0$ . In practice, however, truncation error sets in after about 50 iterations and  $W_{50}$  is not orthogonal to  $W_1$ . The  $W_i$  do remain orthogonal in a "local" sense in that  $W_{50}$  is orthogonal to  $W_{25} - W_{75}$ . Platzman (1975) has shown that the "local" **orthogonality** is adequate for determining periods and structures of at least the lowest modes.

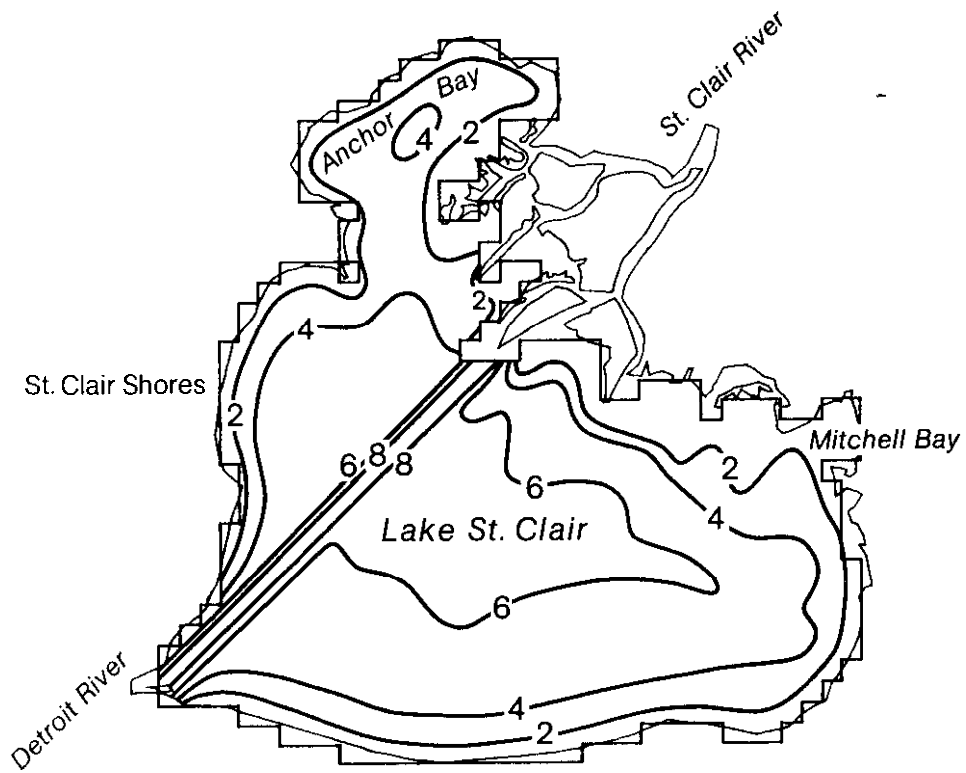


Figure 1.--Numerical grid for Lake St. Clair. Depth contours at 2-m intervals.

In the case of Lake St. Clair, the procedure was truncated at 244, 488, and 731  $W_i$ . A large number of  $W_i$  are required to resolve the modal structures, but the **eigenfrequencies** are determined quite well even at low truncation. At higher truncations the loss of orthogonality tends to cause spurious values of  $\lambda_i$  to appear. These can be recognized in two ways. First, the lowest **eigenvalues** are well determined at low truncation, so that if a new **eigenvalue** appears at a higher truncation limit, it is probably spurious. Second, we can test the structure of the free mode as constructed by (13) with the parameter  $\epsilon$  defined as follows:

$$\epsilon = \int (\nabla \cdot h \nabla \eta_n - \lambda_n \eta_n)^2 dA / \int \eta_n^2 dA. \quad (28)$$

Analytically  $\epsilon$  is zero, but when the **discretized** version of (28) is calculated numerically,  $\epsilon$  is some small number and tends to be higher for spurious **eigenvalues**.

Table 1 lists the lowest 10 frequencies determined by the Lanczos procedure at the three different truncations. The value of  $\epsilon$  at truncation 731 is also shown. Spurious eigenvalues are marked by asterisks. The lowest four frequencies remain constant to five significant figures for the three different truncations. The fifth mode frequency changes in the second significant figure.

The spatial structures of the five lowest modes are shown in Figs. 2-6. The contour interval is 10 percent of the maximum value. The lowest mode, in Fig. 2, with a period of 4.06 h shows maximum amplitude in the Anchor Bay region north of the main lake basin. The nodal line runs across the lake from the St. Clair river inflow to the St. Clair Shores region. On the eastern end of the lake, the amplitude attains only 20 percent of its maximum value.

The second mode, shown in Fig. 3, has a period of 3.12 h. There are two nodal lines so that the oscillation in the northern reaches of Anchor Bay is in phase with the eastern end of the main basin where maximum amplitude occurs. This mode is probably more important than the lowest mode in the generation of storm surges since the predominant westerly wind would pile water up at the eastern shore, conforming to the structure of this mode.

The 2.17-h mode in Fig. 4 also has two nodal lines, but the axis of oscillation is oriented north-to-south. The 1.89-h mode in Fig. 5 is the fundamental oscillation of Mitchell Bay. Note that this mode has a very small space scale and requires a fine grid mesh for sufficient resolution. The fifth mode in Fig. 6 at 1.74h involves the whole Lake St. Clair Basin.

## 5. CONCLUSION

The Lanczos procedure is able to provide more detailed normal mode structures than traditional methods because it is more efficient in terms of computer storage. This was demonstrated on a 1200-m grid representation of Lake St. Clair involving 731 grid squares. The structures of the five lowest modes show detail that could not be resolved on a coarser grid.

Table 1.--Frequencies of oscillation of Lake St. Clair as determined by the Lanczos procedure at various truncations. Frequencies are in cycles per hour. Asterisks denote spurious eigenvalues as explained in the text.

Mode	Truncation			$\epsilon$
	244	488	731	
1	<b>0.24619</b>	<b>0.24619</b>	<b>0.24619</b>	7.99 x 10 <sup>-31</sup>
2	0.32000	0.32000	0.32000	1.95 x 10 <sup>-31</sup>
3	0.45985	0.45985	0.45985	2.26 x 10 <sup>-31</sup>
4	0.52949	0.52949	0.46388"	3.54 x 10 <sup>-15</sup>
5	0.59269	0.57374	0.52949	5.53 x 10 <sup>-31</sup>
6	0.60725	<b>0.59464*</b>	<b>0.55362*</b>	3.18 x 10 <sup>-14</sup>
7	0.63336	0.60640	0.57374	<b>8.16 x 10<sup>-28</sup></b>
8	0.68462	0.61965	0.60640	5.39 x 10 <sup>-27</sup>
9	0.74091	0.68302"	0.61965	3.84 x 10 <sup>-26</sup>
10	0.77816	0.68385	0.68385	8.11 x 10 <sup>-29</sup>

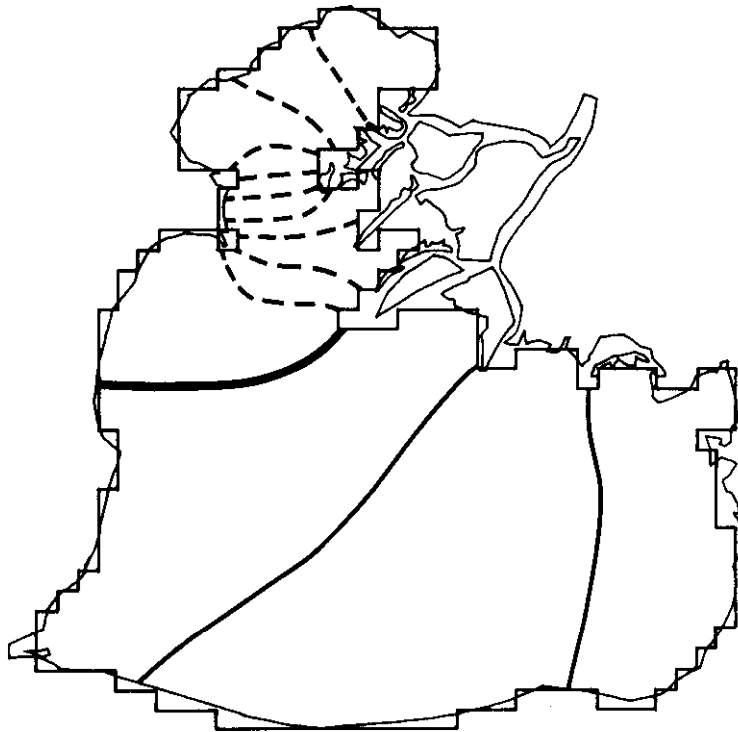


Figure Z.--Amplitude distribution for the first normal mode of Lake St. Clair, with a period of 4.06 h.

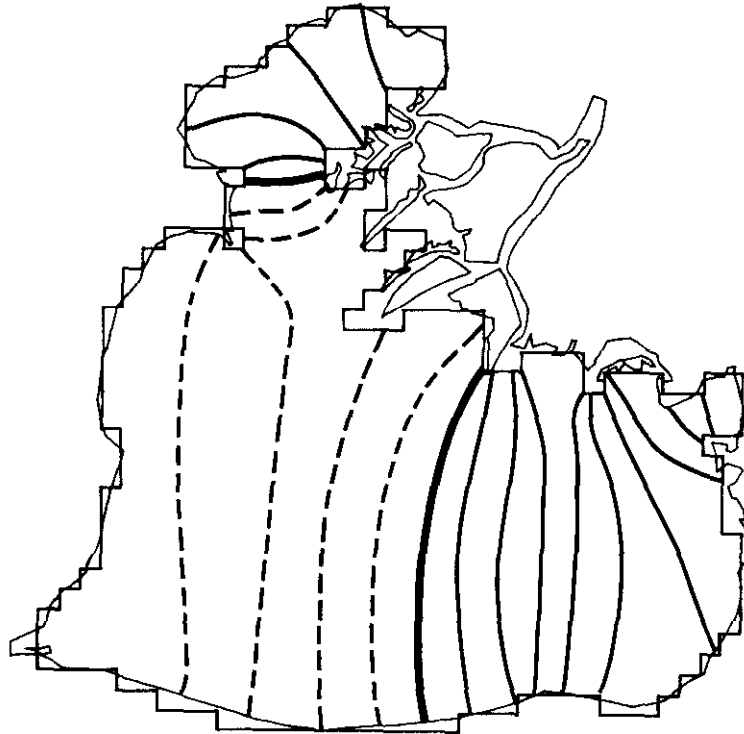


Figure 3.--Amplitude **distribution** for **the second normal mode** of **Lake St. Clair**,  
with a period of 3.12 h.



Figure 4.--Amplitude **distribution** for **the third normal mode** of **Lake St. Clair**,  
with a period of 2.17 h.



**Figure 5.--Amplitude distribution for the fourth normal mode of Lake St. Clair, with a period of 1.89 h.**



**Figure 6.--Amplitude distribution for the fifth normal mode of**

*St. Clair,*

**with a period of 1.74 h.**

## 6. REFERENCES

- Lanczos, C. (1950): An iteration method for the solution of the eigenvalue problem of linear differential and integral operators. *J. Res. Natl. Bur. Stand.* 45:255-282.
- Paige, C. C. (1972): Computational variants of the Lanczos method for the eigenproblem. *J. Inst. Math. Appl.* 10:373-381.
- Platzman, G. W. (1975): Normal modes of the Atlantic and Indian Oceans. *J. Phys. Oceanog.* 5:201-221.
- Smith, B. T. et al. (1974): **Matrix eigenstystem routines--EISPACK guides, Lecture notes in computer science**, Vol 6, G. Goos and J. Hartmanis eds., Berlin, Springer, 387 pp.